
THE ISCHEMIC PENUMBRA

Edited by

Geoffrey A. Bonman

Jean-Cluude Baron

Stephen M. Davis

Frank R. Sharp

840
841
842
843
844
845
846
847
848
849
850
851
852
853
854
855
856
857
858
859
860
861
862
863
864
865
866
867
868
869
870
871
872
873
874
875
876
877
878
879
880
881
882
883
884
885
886
887
888
889
890
891
892
893
894
895

16c. Arterial Spin Labeling

John A. Detre

Department of Neurology, University of Pennsylvania, Pennsylvania, U.S.A.

Philadelphia

Timothy Q. Duong

Department of Neurology, Emory University, Atlanta, Georgia, U.S.A.

Yerkes Imaging Center, Division of Neuroscience and

Although ischemic penumbra can be operationally defined in many ways, the earliest definitions considered thresholds in the reduction of cerebral blood flow (CBF) in the ischemic core and surrounding regions (1). While the ischemic penumbra can now be defined by cellular and molecular events, hypoperfusion remains the proximate cause of cerebral ischemia and a critical physiological parameter in its mechanism. The concept of ischemic thresholds is also universally recognized to have a temporal component—shorter the durations of reversibility occurring in regions, greater the reductions in CBF (2). Accordingly, serial measurements of CBF are ideally required to fully characterize the relationships between CBF and ischemic outcomes, both clinically and in experimental models. Q1

Arterial spin-labeled (ASL) perfusion MRI provides a completely noninvasive method for quantification of CBF, using magnetically labeled arterial blood–water as an endogenous and nominally diffusible flow tracer (3). It is conceptually analogous to the CBF measurements made with $^{15}\text{O}\text{-H}_2\text{O}$ and positron emission tomography (PET) scanning, except that no exogenous or radioactive tracer is required. Instead, radiofrequency (RF) excitation is used to alter the magnetization of arterial blood–water proximal to the tissue of interest; for CBF, arterial blood–water is typically labeled at the base of the brain or in the neck. Another major difference is that ^{15}O decays with a half-life of two minutes, whereas ASL blood–water decays with T1, which is on the order of one to two seconds, depending on the field strength and tissue type. ASL perfusion MRI measurements can, therefore, be made quickly, and rapid changes in CBF can be followed. Although ASL only produces an approximately 1% change in magnetization of the brain, this effect can be reliably measured using modern imaging equipment.

Because ASL is completely noninvasive and the ASL “tracer” is extremely short-lived, it can also be repeated indefinitely. This is a unique difference from other methods for CBF imaging, where repeatability is limited by either radiation dose limits in radionuclide methods or accumulation of the tracer for vascular contrast methods such as dynamic susceptibility contrast (DSC) based perfusion MRI. ASL perfusion MRI is also directly quantifiable in classical units of tissue perfusion ($\text{mL}/\text{g}/\text{min}$) with measurements, knowledge, or assumptions about the labeling efficiency, arterial transit time from the labeling location to the tissue of interest, and T1 relaxation rates in blood and tissue. Modifications of ASL imaging sequences also allow an arterial transit time to be calculated (4). This measure may have physiological significance independent of CBF, potentially indicating the recruitment of collateral flow pathways.

The earliest models for quantifying CBF, based on ASL data, used a modification of the Block equations for longitudinal magnetization with added terms for the delivery of labeled spins by CBF and their removal by venous outflow (3). A well-mixed compartment was also assumed, allowing the venous concentration of label to be replaced with the brain concentration adjusted by the blood:brain partition coefficient for water following the Kety–Schmitt model. Subsequent models for quantifying CBF have also considered an arterial blood–water compartment (5) and finite permeability of water (6).

Several approaches exist for carrying out ASL. They fall into two main categories: pulsed ASL (PASL), which uses a spatially localized RF excitation to saturate or invert the arterial magnetization with respect to the tissue magnetization (7–9,9a), and continuous ASL (CASL) (10), Q2 which uses a velocity-driven adiabatic excitation (11) to invert spins flowing through a designated labeling plane (Fig. 1). In the theoretical limit, CASL methods provide over two-fold F1 greater labeling than PASL methods, though in practice the relative improvement tends to be

896
897
898
899
900
901
902
903
904
905
906
907
908
909
910
911
912
913
914
915
916
917
918
919
920
921
922
923
924
925
926
927
928
929
930
931
932
933
934
935
936
937
938
939
940
941
942
943
944
945
946
947
948
949
950
951

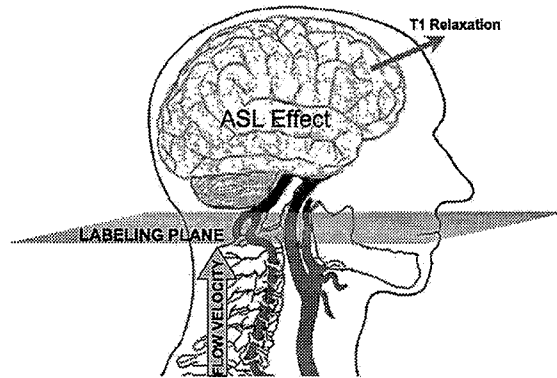


FIGURE 1 A schematic diagram illustrating continuous arterial spin labeling. Velocity-driven adiabatic fast passage inverts arterial blood-water flowing towards the brain as it passes through the labeling plane. The resulting arterial blood-water has opposite magnetization to the static brain water and produces a small decrease in magnetic resonance imaging signal that is measured by comparison with a control condition without arterial spin labeling. The regional magnitude of this signal changes is dependent on cerebral blood flow, which delivers labeled spins to the region, and T1 relaxation, which causes the label to decay. *Abbreviation:* ASL, arterial spin labeling. *Source:* From Refs. 10 and 11.

somewhat less (9,9a). Several methods for selective labeling of individual arteries have also been developed. Some are based on the use of separate small RF coils (12,13), whereas others rely on gradient-based localization (14–16). The ability to selectively label individual arteries is unique to ASL among noninvasive CBF imaging techniques. Q2

ASL was initially reported in the early 1990s for single slices, and CBF measurements were validated against other approaches including flowmeter (17), microspheres (18), hydrogen clearance (19), autoradiographic methods (20), and ^{15}O -PET CBF (21,21a,22). However, several key methodological advances have greatly improved the utility of ASL perfusion MRI. The introduction of a postlabeling delay (5) to allow labeled blood-water to move from the arterial circulation into the microcirculation and tissue greatly reduced the dependency of calculated CBF on variations in arterial transit time and produced CBF images that were far less contaminated by artifacts due to residual label in large arteries that were present in early studies (23). Improved spatial localization for PASL and strategies to control for the spatially dependent off-resonance effects of CASL (24) have permitted multislice ASL, which is necessary for clinical applications and beneficial for research applications. The increased signal strength and prolongation of T1 relaxation rates with increased magnetic field strength act in tandem to greatly improve the sensitivity of high-field ASL (25). The use of surface coils and parallel imaging also increased the sensitivity of ASL methods (26). Finally, under certain circumstances, it is possible to suppress the magnetization from static brain-water, which amplifies the ASL effect from approximately 1% to up to 100% of the measured signal (21,21a). Taken together, these methodological advances have resulted in a 10-fold improvement in the sensitivity of ASL over the past decade. An example of a current ASL perfusion MRI study from human brain is shown in Figure 2. Continued methodological development is focusing on improving labeling efficiency and optimizing strategies for measuring the ASL effect in brain and other organs. Q2
F2

Over the past decade, several studies in animal models and human patients have also established the utility of ASL perfusion MRI for measuring CBF in cerebrovascular disease and stroke. ASL has been used for serial imaging of CBF in animal models (27–29). Brain tissue with perfusion deficits below a critical threshold (2) experiences metabolic energy failure, membrane depolarization, and subsequent cytotoxic edema. These changes precipitate a reduction in the apparent diffusion coefficient (ADC) of brain-water (30), which has been well characterized in animal models of stroke. During the acute phase, the area of ADC abnormality is typically smaller relative to the area of perfusion deficit. As ischemia evolves, most of this ADC abnormality expands and, eventually, coincides with the area of perfusion deficit. The difference in the abnormal region defined by the abnormal perfusion and diffusion contrast in acute stroke is referred to as the “perfusion-diffusion” mismatch, and represents potentially salvageable tissue corresponding to the “ischemic penumbra.” An example of the application of ASL perfusion MRI in a rat stroke model is shown in Figure 3. F3

Critical CBF and ADC thresholds below which infarctions are destined to develop can be defined by correlation with endpoint histology (29). Although there are limitations of this approach, it provides a simple and practical means to define the ischemic penumbra and

952
953
954
955
956
957
958
959
960
961
962
963
964
965
966
967
968
969
970
971
972
973
974
975
976
977
978
979
980
981
982
983
984
985
986
987
988
989
990
991
992
993
994
995
996
997
998
999
1000
1001
1002
1003
1004
1005
1006
1007

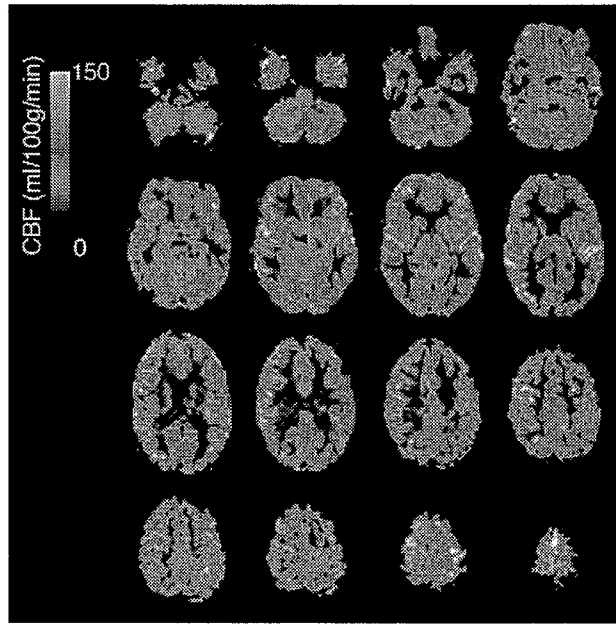


FIGURE 2 Multislice continuous arterial spin labeling perfusion magnetic resonance imaging obtained at 3 T from a normal volunteer in approximately 10 minutes with spinecho echoplanar imaging. *Abbreviation:* CBF, cerebral blood flow.

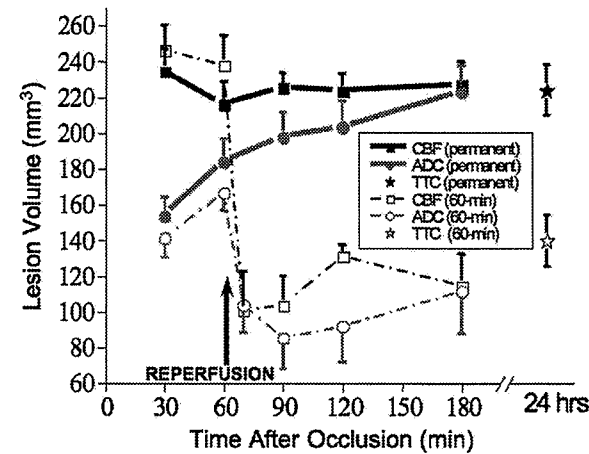
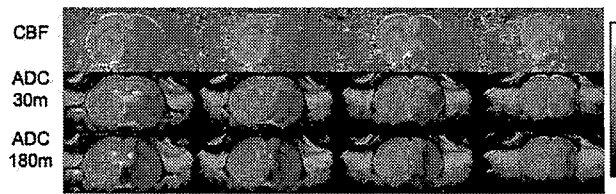


FIGURE 3 (Top) Cerebral blood flow (CBF) maps at 30 minutes, apparent diffusion coefficient maps at 30 and 180 minutes after permanent middle cerebral artery occlusion. CBF was measured using continuous arterial spin labeling (ASL) with a separate neck coil for ASL. Gray scale indicates CBF ranging from 0 to 1 mL/g/min and apparent diffusion coefficient (ADC) ranging from 0 to 1×10^{-3} mm²/sec. (Bottom) Evolution of ADC- and CBF-defined lesion volumes for permanent ($n = 6$) and 60-minute ($n = 6$) stroke. CBF-defined lesion volume of the permanent stroke was constant, whereas ADC-defined lesion volume of the permanent stroke grew bigger with time. Reperfusion salvaged substantial tissues, and some of these tissues showed delayed cell death, as indicated by gradual increase in ADC lesion volume over time after reperfusion. Final infarct volumes were obtained by triphenyl tetrazolium chloride histology at 24 hours after ischemia. *Abbreviations:* ADC, apparent diffusion coefficient; CBF, cerebral blood flow; TTC, triphenyl tetrazolium chloride.

1008
1009
1010
1011
1012
1013
1014
1015
1016
1017
1018
1019
1020
1021
1022
1023
1024
1025
1026
1027
1028
1029
1030
1031
1032
1033
1034
1035
1036
1037
1038
1039
1040
1041
1042
1043
1044
1045
1046
1047
1048
1049
1050
1051
1052
1053
1054
1055
1056
1057
1058
1059
1060
1061
1062
1063

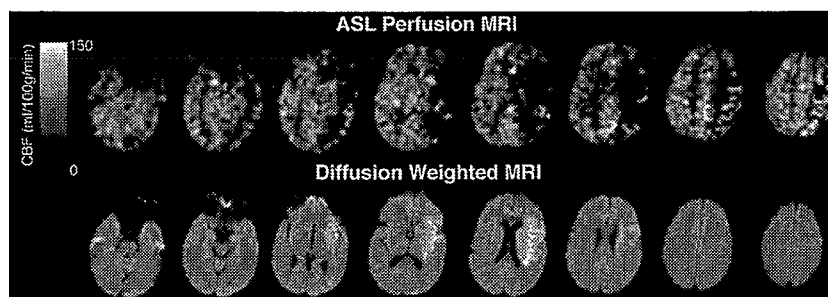


FIGURE 4 Continuous arterial spin-labeled (ASL) perfusion magnetic resonance imaging (MRI) and diffusion-weighted MRI (DWI) obtained at 1.5 T from a 56-year-old man with hemiparesis due to carotid dissection six hours after symptom onset. DWI shows cytotoxic injury primarily around insular cortex, whereas perfusion MRI shows hypoperfusion in affecting most of the middle cerebral artery distribution, suggesting a large penumbral zone. However, owing to the weak ASL effect in the hypoperfused region, cerebral blood flow (CBF) values are difficult to distinguish from zero. High-field ASL should dramatically increase ASL sensitivity for low CBF values. *Abbreviations:* ASL, arterial spin labeling; CBF, cerebral blood flow; MRI, magnetic resonance imaging.

infarcted tissues at different time points after stroke. This approach has also been used to study the effects of reperfusion (31,31a) and other therapeutic interventions (32). For example, the data shown in Figure 3 suggest that about half of the penumbral tissue was salvaged when reperfusion was performed 60 minutes after occlusion, compared with no reperfusion. One limitation of extending this approach to the clinic is that CBF and ADC critical thresholds are defined at one single time point after stroke onset, while it is well known that the duration of CBF reduction should also be taken into account (2). Objective classification of ischemic penumbra, normal, and infarcted tissues (such as using automated clustering algorithm based on multispectral CBF, ADC, and other MRI data) is clearly important and has been demonstrated in stroke models (31,31a) and to some extent in humans (33). Q2

In human patients with acute stroke and chronic cerebrovascular disease, ASL perfusion MRI has been used to demonstrate the presence of chronic asymptomatic and symptomatic hypoperfusion (34–36). Although these studies have demonstrated the feasibility of using ASL to characterize the ischemic penumbra, accurate measurement of low CBF values has remained challenging because signal changes are particularly small and arterial transit times can be significantly longer than T1 of arterial blood–water. However, most of the existing data on ASL in experimental and clinical stroke were acquired at 1.5 T using early methodology, with several-fold lower sensitivity than that is now available. The recent improvements in ASL methodology described earlier should facilitate the transition of ASL perfusion MRI from feasibility to practical utility in basic and clinical research on the ischemic penumbra. Q2

REFERENCES

1. Astrup J, Siesjo BK, Symon L. Thresholds in cerebral ischemia - the ischemic penumbra. *Stroke* 1981; 12:723–725.
2. Hossmann KA. Viability thresholds and the penumbra of focal ischemia. *Ann Neurol* 1994; 36(4):557–565.
3. Detre JA, Leigh JS, Williams DS, Koretsky AP. Perfusion imaging. *Magn Reson Med* 1992; 23:37–45.
4. Wang J, Alsop DC, Song HK, et al. Arterial transit time imaging with flow encoding arterial spin tagging (FEAST). *Magn Reson Med* 2003; 50(3):599–607.
5. Alsop DC, Detre JA. Reduced transit-time sensitivity in noninvasive magnetic resonance imaging of human cerebral blood flow. *J Cereb Blood Flow Metab* 1996; 16:1236–1249.
6. Parkes LM, Tofts PS. Improved accuracy of human cerebral blood perfusion measurements using arterial spin labeling: accounting for capillary water permeability. *Magn Reson Med* 2002; 48(1):27–41.
7. Edelman RR, Siewert B, Darby DG, et al. Qualitative mapping of cerebral blood flow and functional localization with echo-planar MR imaging and signal targeting with alternating radio frequency. *Radiology* 1994; 192:513–520.
8. Kim SG, Tsekos NV. Perfusion imaging by a flow-sensitive alternating inversion recovery (FAIR) technique: application to functional brain imaging. *Magn Reson Med* 1997; 37(3):425–435.

- 1064 9. Wong EC, Buxton RB, Frank LR. A theoretical and experimental comparison of continuous and
1065 pulsed arterial spin labeling techniques for quantitative perfusion imaging. *Magn Reson Med* 1998; Q2
1066 40:348–355.
- 1067 9a. Wong EC, Buxton RB, Frank LR. Quantitative imaging of perfusion using a single subtraction
1068 (QUIPSS and QUIPSS II). *Magn Reson Med* 1998; 39:702–708. Q2
- 1069 10. Williams DS, Detre JA, Leigh JS, Koretsky AP. Magnetic resonance imaging of perfusion using spin
1070 inversion of arterial water. *Proc Natl Acad Sci USA* 1992; 89:212–216.
- 1071 11. Sardashti M, Schwartzberg DG, Stomp GP, Dixon WT. Spin labeling angiography of the carotids by
1072 presaturation and simplified adiabatic inversion. *Magn Reson Med* 1990; 15:192–200.
- 1073 12. Detre JA, Zhang W, Roberts DA, et al. Tissue specific perfusion imaging using arterial spin labeling.
1074 *NMR Biomed* 1994; 7:75–82.
- 1075 13. Zaharchuk G, Ledden PJ, Kwong KK, Reese TG, Rosen BR, Wald LL. Multislice perfusion and perfu-
1076 sion territory imaging in humans with separate label and image coils. *Magn Reson Med* 1999;
1077 41:1093–1098.
- 1078 14. Hendrikse J, van der Grond J, Lu H, van Zijl PC, Golay X. Flow territory mapping of the cerebral
1079 arteries with regional perfusion MRI. *Stroke* 2004; 35(4):882–887.
- 1080 15. Werner R, Norris DG, Alfke K, Mehdorn HM, Jansen O. Continuous artery-selective spin labeling
1081 (CASSL). *Magn Reson Med* 2005; 53(5):1006–1012.
- 1082 16. Jones CE, Wolf RL, Detre JA, et al. Structural MRI of carotid artery atherosclerotic lesion burden
1083 and characterization of hemispheric cerebral blood flow before and after carotid endarterectomy. *NMR
1084 Biomed* 2006; 19(2):198–208.
- 1085 17. Williams DS, Grandis DJ, Zhang W, Koretsky AP. Magnetic resonance imaging of perfusion in the
1086 isolated rat heart using spin inversion of arterial water. *Magn Reson Med* 1993; 30(3):361–365.
- 1087 18. Walsh EG, Minematsu K, Leppo J, Moore SC. Radioactive microsphere validation of a volume
1088 localized continuous saturation perfusion measurement. *Magn Reson Med* 1993; 31:147–153.
- 1089 19. Pell GS, King MD, Proctor E, et al. Comparative study of the FAIR technique of perfusion quantifica-
1090 tion with the hydrogen clearance method. *J Cereb Blood Flow Metab* 2003; 23(6):689–699.
- 1091 20. Ewing JR, Cao Y, Knight RA, Fenstermacher JD. Arterial spin labeling: validity testing and comparison
1092 studies. *J Magn Reson Imaging* 2005; 22(6):737–740.
- 1093 21. Ye FQ, Berman KF, Ellmore T, et al. H(2)(15)O PET validation of steady-state arterial spin tagging Q2
1094 cerebral blood flow measurements in humans. *Magn Reson Med* 2000; 44(3):450–456.
- 1095 21a. Feng C M, Narayana S, Lancaster JL, et al. CBF changes during brain activation: fMRI vs. PET. Q2
1096 *Neuroimage* 2004; 22(1):443–446.
- 1097 22. Ye FQ, Frank JA, Weinberger DR, McLaughlin AC. Noise reduction in 3D perfusion imaging by
1098 attenuating the static signal in arterial spin tagging (ASSIST). *Magn Reson Med* 2000; 44(1):92–100.
- 1099 23. Roberts DA, Detre JA, Bolinger L, Insko EK, Leigh JS Jr. Quantitative magnetic resonance imaging of
1100 human brain perfusion at 1.5 T using steady-state inversion of arterial water. *Proc Natl Acad Sci
1101 USA* 1994; 91:33–37.
- 1102 24. Alsop DC, Detre JA. Multisection cerebral blood flow MR imaging with continuous arterial spin
1103 labeling. *Radiology* 1998; 208:410–416.
- 1104 25. Wang J, Alsop DC, Li L, et al. Comparison of quantitative perfusion imaging using arterial spin
1105 labeling at 1.5 and 4.0 Tesla. *Magn Reson Med* 2002; 48(2):242–254.
- 1106 26. Wang Z, Wang J, Connick TJ, Wetmore GS, Detre JA. Continuous ASL perfusion MRI with an array
1107 coil and parallel imaging at 3T. *Magn Reson Med* 2005; 54(3):732–737.
- 1108 27. Hoehn-Berlage M, Norris DG, Kohno K, Mies G, Leibfritz D, Hossmann KA. Evolution of regional
1109 changes in apparent diffusion coefficient during focal ischemia of rat brain: the relationship of quan-
1110 titative diffusion NMR imaging to reduction in cerebral blood flow and metabolic disturbances.
1111 *J Cereb Blood Flow Metab* 1995; 15(6):1002–1011.
- 1112 28. Lythgoe MF, Thomas DL, Calamante F, et al. Acute changes in MRI diffusion, perfusion, T(1), and
1113 T(2) in a rat model of oligemia produced by partial occlusion of the middle cerebral artery. *Magn
1114 Reson Med* 2000; 44(5):706–712.
- 1115 29. Shen Q, Meng X, Fisher M, Sotak CH, Duong TQ. Pixel-by-pixel spatiotemporal progression of focal
1116 ischemia derived using quantitative perfusion and diffusion imaging. *J Cereb Blood Flow Metab*
1117 2003; 23(12):1479–1488.
- 1118 30. Moseley ME, Cohen Y, Mintotovitch J, et al. Early detection of regional cerebral ischemia in cats:
1119 comparison of diffusion- and T2-weighted MRI and spectroscopy. *Magn Reson Med* 1990;
1120 14:330–346.
- 1121 31. Shen Q, Fisher M, Sotak CH, Duong TQ. Effects of reperfusion on ADC and CBF pixel-by-pixel
1122 dynamics in stroke: characterizing tissue fates using quantitative diffusion and perfusion imaging. Q2
1123 *J Cereb Blood Flow Metab* 2004; 24(3):280–290.
- 1124 31a. Shen Q, Ren H, Fisher M, Bouley J, Duong TQ. Dynamic tracking of acute ischemic tissue fates using
1125 improved unsupervised ISODATA analysis of high-resolution quantitative perfusion and diffusion
1126 data. *J Cereb Blood Flow Metab* 2004; 24(8):887–897.
- 1127 32. Bardutzky J, Meng X, Bouley J, Duong TQ, Ratan R, Fisher M. Effects of intravenous dimethyl sulf- Q2
1128 oxide on ischemia evolution in a rat permanent occlusion model. *J Cereb Blood Flow Metab* 2005;
1129 25(8):968–977.

- 1121 33. Wu O, Koroshetz WJ, Ostergaard L, et al. Predicting tissue outcome in acute human cerebral ischemia using combined diffusion- and perfusion-weighted MR imaging. *Stroke* 2001; 32(4):933–942.
- 1122
- 1123 34. Detre JA, Alsop DC, Vives LR, Maccotta L, Teener JW, Raps EC. Noninvasive MRI evaluation of cerebral blood flow in cerebrovascular disease. *Neurology* 1998; 50:633–641.
- 1124
- 1125 35. Chalela JA, Alsop DC, Gonzalez-Atavalez JB, Maldjian JA, Kasner SE, Detre JA. Magnetic resonance perfusion imaging in acute ischemic stroke using continuous arterial spin labeling. *Stroke* 2000; 31:680–687.
- 1126
- 1127 36. Jefferson AL, Glosser G, Detre JA, Sinson G, Liebeskind DS. Neuropsychological and perfusion MR imaging correlates of revascularization in a case of moyamoya syndrome. *AJNR Am J Neuroradiol* 2006; 27(1):98–100.
- 1128
- 1129
- 1130
- 1131
- 1132
- 1133
- 1134
- 1135
- 1136
- 1137
- 1138
- 1139
- 1140
- 1141
- 1142
- 1143
- 1144
- 1145
- 1146
- 1147
- 1148
- 1149
- 1150
- 1151
- 1152
- 1153
- 1154
- 1155
- 1156
- 1157
- 1158
- 1159
- 1160
- 1161
- 1162
- 1163
- 1164
- 1165
- 1166
- 1167
- 1168
- 1169
- 1170
- 1171
- 1172
- 1173
- 1174
- 1175
- 1176